

# Fluorescence characteristics of six 4,7-disubstituted benzofurazan compounds: an experimental and semi-empirical MO study



Seiichi Uchiyama, Tomofumi Santa and Kazuhiro Imai\*

Graduate School of Pharmaceutical Sciences, The University of Tokyo, 7-3-1 Hongo, Bunkyo-ku, Tokyo, 113-0033, Japan

Received (in Cambridge, UK) 22nd June 1999, Accepted 1st September 1999

To elucidate the factors which determine the fluorescence characteristics (fluorescence quantum yield ( $\Phi$ ), maximum excitation/absorption and emission wavelengths) of 4,7-disubstituted benzofurazan compounds, we have studied the excitation and emission (or relaxation) processes of six typical 4,7-disubstituted benzofurazan compounds. The absorption and fluorescence spectra of these compounds were measured in twenty different solvents and the molecular orbitals relating to excitation and emission (or relaxation) were calculated with semi-empirical methods. The absorption/excitation and emission were ascribed to the electronic transition between HOMO and LUMO. The order of energy gaps between HOMO and LUMO of the 4,7-substituted benzofurazan compounds at the optimized geometry of the ground state agreed with the order of the maximum absorption/excitation energy in vapor phase obtained with the Taft–Kamlet treatment. The order of energy gaps at the optimized geometry of the excited state also agreed with the order of the maximum emission energy in the vapor phase obtained with the Taft–Kamlet treatment. The energy levels of the  $S_1$  state of the 4,7-disubstituted benzofurazan compounds were just under the energy level of the  $T_2$  state. The order of the energy gaps between the  $S_1$  state and the  $T_2$  state of the 4,7-disubstituted benzofurazan compounds agreed with the order of the fluorescence quantum yield ( $\Phi$ ) in cyclohexane. These results show that the maximum absorption/excitation, emission wavelengths and the fluorescence quantum yields ( $\Phi$ ) of the 4,7-disubstituted benzofurazan compounds are determined by the energy gaps between the HOMO and LUMO energy at the geometry of the ground state, of the excited state and the energy gap between the  $S_1$  and  $T_2$  states, respectively.

## Introduction

There have been many reports on the effects of the skeleton<sup>1–3</sup> and the substituent groups<sup>4–11</sup> of molecules on the fluorescence characteristics (maximum excitation wavelength, maximum emission wavelength and fluorescence quantum yield ( $\Phi$ )), yet the general relationships between the fluorescence characteristics (especially the fluorescence quantum yield ( $\Phi$ )) and the chemical structure have not hitherto been revealed. To clarify the general relationships between the chemical structure and the fluorescence characteristics is of great value in the fields of analytical and biological chemistry, since such relationships allow us to design useful fluorescent derivatization reagents and probes.

In the course of our studies on the development of fluorescent derivatization reagents having the benzofurazan (2,1,3-benzoxadiazole) skeleton with high fluorescence quantum yields ( $\Phi$ ) and long emission wavelengths, the following compounds were synthesized: 4-fluoro-7-nitro-2,1,3-benzoxadiazole (NBD-F)<sup>12</sup> for amines, 4-(*N,N*-dimethylaminosulfonyl)-7-fluoro-2,1,3-benzoxadiazole (DBD-F)<sup>13</sup> for amines and thiols, 4-aminosulfonyl-7-fluoro-2,1,3-benzoxadiazole (ABD-F),<sup>14</sup> 7-fluoro-2,1,3-benzoxadiazole-4-sulfonate (SBD-F)<sup>15</sup> for thiols, 4-(*N*-hydrazinoformylmethyl-*N*-methyl)amino-7-(*N,N*-dimethylaminosulfonyl)-2,1,3-benzoxadiazole (DBD-CO-Hz)<sup>16</sup> and 4-(*N*-hydrazinoformylmethyl-*N*-methyl)amino-7-nitro-2,1,3-benzoxadiazole (NBD-CO-Hz)<sup>17</sup> for carboxylic acids. We also investigated the effects of the substituent groups at the 4- and 7-positions on the fluorescence characteristics of the benzofurazan compounds and found that the fluorescence characteristics of these compounds were related to the sum and the difference of the Hammett substituent constants ( $\sigma_p$ ) of the substituent groups at the 4- and 7-positions.<sup>18</sup> The sum and the difference of  $\sigma_p$  were assumed to correspond to the total electron density of the benzofurazan skeleton and the dipole

moment directed from the 4- to the 7-position, respectively. Therefore, the LUMO energy reflecting the total electron density of the benzofurazan skeleton and the dipole moment directed from the 4- to the 7-position obtained with PM3 calculations were employed as new parameters, and the relationship between these new parameters and the fluorescence characteristics of 4,7-disubstituted benzofurazan compounds was studied. The empirical relationship enabled us to predict the fluorescence characteristics from the chemical structures of 4,7-disubstituted benzofurazan compounds.<sup>19</sup>

The present project is focussed on the clarification of the theoretical relationship between the fluorescence characteristics and the chemical structures of 4,7-disubstituted benzofurazan compounds based on the study of the excitation and emission (or relaxation) processes and the energy levels of these molecules. There have only been a few reports on the excitation and emission processes of benzofurazan compounds,<sup>20–22</sup> and the substituent groups discussed in these papers were limited to only the nitro and amino groups.

In this paper, we study the ground ( $S_0$ ) state and first excited singlet ( $S_1$ ) state of six 4,7-disubstituted benzofurazan compounds (Fig. 1, (1)–(6) with different fluorescence characteristics using solvent effects on the absorption and fluorescence spectra. We have also calculated the molecular orbital relating to excitation and emission (or relaxation) by semi-empirical

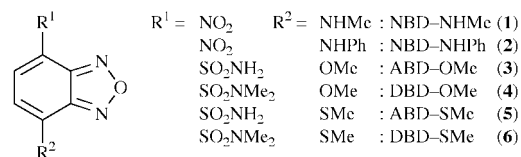
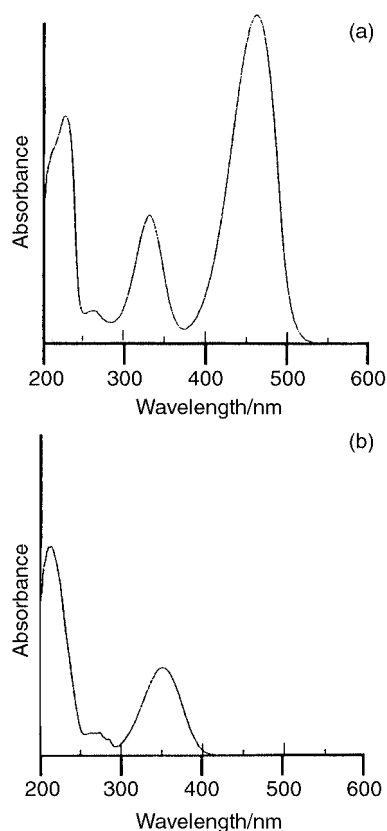


Fig. 1 Chemical structures of 4,7-disubstituted benzofurazan compounds in the present study.

**Table 1** Absorption data of six 4,7-disubstituted benzofuran compounds in twenty solvents

Solvent	Maximum absorption wavelength/nm ( $\epsilon/10^4 \text{ dm}^3 \text{ mol}^{-1} \text{ cm}^{-1}$ )					
	NBD-NHMe (1)	NBD-NHPh (2)	ABD-OMe (3)	DBD-OMe (4)	ABD-SMe (5)	DBD-SMe (6)
<i>n</i> -Hexane	422(1.79)	441(2.00)	342(0.63)	343(0.68)	381(0.98)	379(1.33)
Cyclohexane	425(1.38)	443(1.95)	345(0.34)	346(0.49)	381(0.68)	380(1.23)
Carbon tetrachloride	430(1.86)	447(2.32)	345(0.72)	347(0.75)	382(1.15)	382(1.53)
Diethyl ether	441(2.11)	457(2.45)	343(0.69)	349(0.75)	380(1.14)	384(1.44)
Toluene	442(1.93)	456(2.16)	349(0.64)	352(0.68)	389(1.04)	390(1.26)
Benzene	443(2.00)	457(1.95)	351(0.57)	352(0.59)	388(0.96)	390(1.11)
1,4-Dioxane	448(2.00)	460(2.24)	348(0.61)	350(0.62)	382(0.96)	386(1.15)
Chloroform	446(2.01)	463(2.45)	348(0.64)	351(0.66)	388(1.06)	388(1.21)
Dichloromethane	449(2.27)	464(2.66)	348(0.68)	353(0.72)	389(1.19)	390(1.29)
Ethyl acetate	450(2.14)	464(2.38)	347(0.61)	351(0.66)	384(1.00)	385(1.20)
Tetrahydrofuran	454(2.12)	468(2.31)	350(0.55)	352(0.60)	385(0.93)	388(1.13)
Acetone	456(2.24)	470(2.50)	350(0.65)	351(0.66)	385(0.98)	387(1.25)
Acetonitrile	458(2.30)	469(2.28)	348(0.60)	353(0.68)	385(1.02)	388(1.17)
<i>tert</i> -Butyl alcohol	459(2.20)	470(2.78)	347(0.65)	351(0.73)	383(0.99)	386(1.41)
Propan-2-ol	459(2.35)	472(2.61)	348(0.60)	350(0.71)	385(1.00)	388(1.39)
Ethanol	459(2.48)	472(2.51)	349(0.60)	352(0.69)	384(1.05)	388(1.23)
Methanol	461(2.58)	473(2.56)	348(0.63)	353(0.68)	384(1.02)	389(1.26)
<i>N,N</i> -Dimethylformamide	467(2.20)	487(2.60)	354(0.57)	355(0.64)	390(0.94)	391(1.20)
Dimethyl sulfoxide	474(2.20)	488(2.52)	355(0.52)	357(0.58)	392(0.83)	394(1.03)
Water	478(3.17)	489(2.72)	350(0.66)	355(0.76)	390(1.06)	394(1.04)

**Fig. 2** Absorption spectra of (a) NBD-NHMe (1) and (b) ABD-OMe (3) in methanol.

molecular orbital methods, and discuss the factors which determine the fluorescence characteristics of these compounds (1)–(6).

## Results and discussion

### 1. Excitation process

The absorption spectra of the six 4,7-disubstituted benzofuran compounds in various solvents. The typical absorption spectra of the six 4,7-disubstituted benzofuran compounds are shown in Fig. 2. Among the six 4,7-disubstituted benzo-

furan compounds (1–6), NBD-NHMe (1) and NBD-NHPh (2) have three distinct absorption bands as shown in Fig. 2(a). According to the assignments reported previously for NBD-amino derivatives,<sup>20–22</sup> the short-wavelength band may be related to the aromatic system of the molecule, the intermediate band to a  $\pi \rightarrow \pi^*$  transition polarized along the major axis of the heterocycle, and the intense low energy band to an intramolecular charge transfer (ICT) taking place between the donor group and the nitro acceptor group situated at the 4- and 7-positions, respectively. ABD-OMe (3), DBD-OMe (4), ABD-SMe (5) and DBD-SMe (6) have only two distinct absorption bands as shown in Fig. 2(b), and have no bands at wavelengths longer than 420 nm. In this paper, the excitation corresponding to the lowest energy band of six 4,7-disubstituted benzofuran compounds (1–6) was studied in order to investigate the excitation process from the ground state to the first excited state.

The maximum absorption wavelengths and the molecular extinction coefficients ( $\epsilon$ ) of the six 4,7-disubstituted benzofuran compounds in 20 different solvents are summarized in Table 1. The maximum absorption wavelengths of NBD derivatives 1 and 2 were longer than those of ABD and DBD derivatives 3–6. These results agreed with the previous reports<sup>23,24</sup> that compounds having strong electron donating and strong electron accepting substituent groups were excited at the long wavelength (the order of electron donating ability is NHMe, NHPh > OMe, SMe and of electron accepting ability is  $\text{NO}_2 > \text{SO}_2\text{NH}_2, \text{SO}_2\text{NMe}_2$ ). With increasing solvent dipolarity, the maximum absorption wavelengths of NBD derivatives 1 and 2 shifted more bathochromically than those of ABD and DBD derivatives 3–6 and the molar extinction coefficients ( $\epsilon$ ) of NBD derivatives 1 and 2 rose, while  $\epsilon$  of ABD and DBD derivatives 3–6 did not change. These results showed that the lowest vibrational  $S_0$  state has a large polarity in NBD derivatives 1 and 2. On the other hand, as regards ABD and DBD derivatives 3–6, the lowest vibrational  $S_0$  state has a small polarity.

**Taft–Kamlet treatment.** The solvent effects on the maximum absorption wavenumber were studied with the Taft–Kamlet treatment, and the results are summarized in Table 2. The maximum absorption wavelengths of the six 4,7-disubstituted benzofuran compounds in the vapor phase were calculated as 1 424 nm, 2 441 nm, 3 343 nm, 4 346 nm, 5 381 nm and 6 381 nm, respectively. Since the absolute value of coefficient  $s$  shows the polarity in the lowest vibrational  $S_0$  state, the polarity in the

**Table 2** Calculated values of the vapor phase absorption wavenumber  $\nu_0$  and solvatochromic coefficients  $s$ ,  $a$ ,  $b$  and  $d$  expressed in  $10^3 \text{ cm}^{-1}$ , standard error, multiple correlation coefficient  $r$  and number of data points used in the calculation

	$\nu_0$	$s$	$a$	$b$	se	$r$	Data points
NBD-NHMe ( <b>1</b> ) <sup>a</sup>	23.57	-1.83	-0.24	-0.87	0.12	0.989	20
NBD-NHPh ( <b>2</b> ) <sup>a</sup>	22.67	-1.62	-0.12	-0.73	0.12	0.984	20
ABD-OMe ( <b>3</b> ) <sup>a</sup>	29.15	-0.79	0.23	-0.19	0.12	0.908	20
DBD-OMe ( <b>4</b> ) <sup>b</sup>	28.92	-0.85	0.04	—	0.09	0.947	20
ABD-SMe ( <b>5</b> ) <sup>a</sup>	26.27	-0.75	0.09	0.13	0.12	0.884	20
DBD-SMe ( <b>6</b> ) <sup>b</sup>	26.27	-0.85	-0.02	—	0.09	0.950	20

Calculations were performed using <sup>a</sup> eqn. (2) or <sup>b</sup> eqn. (3) to treat the whole set of data.

**Table 3** INDO/S results of excitation process for six benzofurazan compounds

	$\lambda_{\text{ex}}/\text{nm}$	$f$	CI
NBD-NHMe ( <b>1</b> )	409	0.299	HOMO→LUMO(76%) HOMO-4→LUMO+1(7%)
NBD-NHPh ( <b>2</b> )	418	0.325	HOMO→LUMO(74%) HOMO-6→LUMO+1(9%)
ABD-OMe ( <b>3</b> )	372	0.281	HOMO→LUMO(95%)
DBD-OMe ( <b>4</b> )	372	0.284	HOMO→LUMO(95%)
ABD-SMe ( <b>5</b> )	375	0.293	HOMO→LUMO(96%)
DBD-SMe ( <b>6</b> )	375	0.297	HOMO→LUMO(95%)

$f$  = Oscillator strength.

lowest vibrational  $S_0$  state of NBD derivatives **1** and **2** is larger than those of ABD and DBD derivatives **3–6**. The large absolute values of coefficient  $b$  of NBD derivatives **1** and **2** obtained with the Taft–Kamlet treatment indicate that the hydrogen bond donor group (namely  $\text{NH}_2$  and  $\text{NHPh}$  groups) is related to the electronic transition in the absorption process, and suggest that electron flow from the  $\text{NH}_2$  or  $\text{NHPh}$  group to nitrobenzofurazan is associated with the absorption process.

**INDO/S calculation.** The electronic transition of the absorption process of six 4,7-disubstituted benzofurazan compounds was studied by using the INDO/S calculation. The results of the INDO/S calculation for the characteristics of the transition from the lowest vibrational  $S_0$  state to the Franck–Condon state of the compounds **1–6** are summarized in Table 3. The maximum absorption wavelengths obtained with the INDO/S calculation almost agree with those obtained with the Taft–Kamlet treatment. Other strong absorptions could not be obtained with the INDO/S calculation except for the results shown in Table 3. The INDO/S calculation showed that the energy gap between the HOMO and LUMO of 4,7-disubstituted benzofurazan compounds mainly determined the absorption wavelength. In fact, the order of the energy gap between the HOMO and LUMO of the six 4,7-disubstituted benzofurazan compounds at the optimized geometry of the lowest vibrational  $S_0$  state calculated with INDO/S were **3** 6.966 eV > **4** 6.958 eV > **5** 6.902 eV > **6** 6.900 eV > **1** 6.520 eV > **2** 6.402 eV, respectively, and these results agreed with the order of maximum absorption wavenumber in the vapor phase obtained with the Taft–Kamlet treatment (**3** > **4** > **5** = **6** > **1** > **2**). The dipole moments at the Franck–Condon state of the compounds **1–6** were calculated as **1** 12.289 D, **2** 12.966 D, **3** 10.344 D, **4** 10.960 D, **5** 11.010 D and **6** 11.549 D, respectively. The dipole moments at the Franck–Condon state of NBD derivatives **1** and **2** were larger than those of ABD and DBD derivatives **3–6**, because the electron flows from the amino group to the nitrobenzofurazan in the NBD derivatives **1** and **2**, while electron does not flow owing to the weakness of the electron donating ability of methoxy and methylthio groups, or the electron accepting ability of the aminosulfonyl and dimethylaminosulfonyl groups with the ABD and DBD derivatives **3–6**. These results of the INDO/S calculation also indicated that the ICT character in the Franck–

Condon state of NBD derivatives **1** and **2** is stronger than those of ABD and DBD derivatives **3–6**.

## 2. Emission (or relaxation) process

**The fluorescence spectra of the six 4,7-disubstituted benzofurazan compounds in various solvents.** The maximum excitation wavelengths and the fluorescence quantum yields ( $\Phi$ ) of the six 4,7-disubstituted benzofurazan compounds in twenty different solvents are summarized in Table 4. The 4,7-disubstituted benzofurazan compounds were excited at the maximum absorption wavelength and had one distinct fluorescence band. As shown in Table 5, the fluorescence quantum yields ( $\Phi$ ) were very different between these benzofurazan compounds. NBD-NHMe (**1**) and ABD-SMe (**5**) have large fluorescence quantum yields ( $\Phi$ ), ABD-OMe (**3**) and DBD-SMe (**6**) have moderate fluorescence quantum yields ( $\Phi$ ) and NBD-NHPh (**2**) and DBD-OMe (**4**) have small fluorescence quantum yields ( $\Phi$ ). The fluorescence quantum yields ( $\Phi$ ) of the compounds **1**, **2**, **5** and **6** were strongly influenced by the solvents, whereas those of the compounds **3** and **4** were not influenced by the solvents. In particular, the fluorescence quantum yields ( $\Phi$ ) of NBD-NHMe (**1**) and ABD-SMe (**5**) were very low in highly polar solvents like methanol and water. These results suggest that the relaxation might occur from ICT ( $S_1$ ) state to the lower energy, nonemissive twisted intramolecular charge transfer (TICT) state.<sup>22,23,25,26</sup> The maximum emission wavelengths of NBD derivatives **1** and **2** were longer than those of ABD and DBD derivatives **3–6**. In contrast with the maximum absorption wavelengths, the maximum emission wavelengths of all six 4,7-disubstituted benzofurazan compounds shifted bathochromically with increasing solvent dipolarity. These bathochromic shifts indicated that the lowest vibrational  $S_1$  state of six 4,7-disubstituted benzofurazan compounds have ICT character.

**Taft–Kamlet treatment.** The solvent effects on the maximum emission wavenumber were studied with the Taft–Kamlet treatment and the results are summarized in Table 5. The maximum emission wavelength of the six 4,7-disubstituted benzofurazan compounds in the vapor phase were calculated as **1** 499 nm, **2** 514 nm, **3** 431 nm, **4** 438 nm, **5** 471 nm and **6** 463 nm, respectively. The large absolute values of coefficient  $s$  of the six 4,7-disubstituted benzofurazan compounds indicated that the lowest vibrational  $S_1$  states of these compounds have large ICT character. And the large absolute values of coefficient  $a$  of ABD and DBD derivatives **3–6** revealed that the hydrogen bond acceptor groups  $\text{SO}_2\text{NH}_2$ ,  $\text{SO}_2\text{NMe}_2$  are related to the electronic transition of the emission process. The large absolute values of coefficient  $b$  of ABD derivatives **3** and **5** indicated that the hydrogen bond donor group  $\text{SO}_2\text{NH}_2$  is also related with the electronic transition of the emission process. These results suggested that the electron flows from the benzofurazan skeleton to an electron accepting group ( $\text{SO}_2\text{NH}_2$ ,  $\text{SO}_2\text{NMe}_2$ ) in the ABD and DBD derivatives **3–6** with stabilization from the Franck–Condon state to the lowest vibrational  $S_1$  state, hence the lowest vibrational  $S_1$  state of these compounds have large ICT character.

**Table 4** Emission data of six 4,7-disubstituted benzofurazan compounds in twenty solvents

Solvent	Maximum emission wavelength/nm ( $\Phi$ )					
	NBD-NHMe (1)	NBD-NHPh (2)	ABD-OMe (3)	DBD-OMe (4)	ABD-SMe (5)	DBD-SMe (6)
<i>n</i> -Hexane	500(0.086)	515(0.0089)	427(0.031)	434(0.0014)	467(0.35)	459(0.044)
Cyclohexane	499(0.16)	517(0.013)	436(0.040)	447(0.0018)	470(0.80)	460(0.053)
Carbon tetrachloride	502(0.20)	525(0.0032)	439(0.031)	454(0.0011)	471(0.67)	466(0.052)
Diethyl ether	506(0.86)	531(0.000082)	440(0.045)	445(0.00080)	483(0.69)	470(0.049)
Toluene	510(0.53)	532(0.00013)	445(0.052)	448(0.0014)	498(0.39)	487(0.12)
Benzene	511(0.63)	534(0.00011)	448(0.074)	449(0.0015)	497(0.49)	487(0.13)
1,4-Dioxane	517(0.79)	536(0.00012)	452(0.074)	450(0.0011)	496(0.49)	488(0.063)
Chloroform	516(0.74)	539(0.000064)	446(0.060)	452(0.0013)	493(0.42)	486(0.14)
Dichloromethane	512(0.78)	542(0.000014)	446(0.080)	448(0.00098)	501(0.58)	492(0.15)
Ethyl acetate	516(0.79)	541(0.000060)	452(0.065)	452(0.0010)	498(0.35)	488(0.065)
Tetrahydrofuran	516(0.80)	545(0.000067)	452(0.083)	451(0.0013)	495(0.34)	489(0.076)
Acetone	521(0.74)	549(0.00099)	455(0.092)	439(0.0013)	504(0.12)	498(0.057)
Acetonitrile	524(0.38)	548(0.000034)	460(0.097)	458(0.00066)	510(0.17)	502(0.077)
<i>tert</i> -Butyl alcohol	522(0.46)	545(0.00012)	459(0.091)	448(0.0033)	504(0.10)	493(0.056)
Propan-2-ol	521(0.37)	550(0.000071)	463(0.099)	451(0.0024)	507(0.077)	497(0.041)
Ethanol	524(0.31)	551(0.000055)	464(0.097)	456(0.0014)	507(0.049)	502(0.035)
Methanol	528(0.23)	550(0.000059)	469(0.10)	461(0.00099)	513(0.036)	507(0.025)
<i>N,N</i> -Dimethylformamide	527(0.33)	571(0.000018)	464(0.11)	464(0.0010)	505(0.021)	504(0.015)
Dimethyl sulfoxide	532(0.026)	572(0.000042)	471(0.024)	472(0.0011)	513(0.0088)	514(0.0039)
Water	541(0.028)	586(0.000020)	490(0.11)	491(0.00049)	530(0.015)	525(0.019)

**Table 5** Calculated values of the vapor phase emission wavenumber  $\nu_0$  and solvatochromic coefficients  $s$ ,  $a$ ,  $b$  and  $d$  expressed in  $10^3 \text{ cm}^{-1}$ , standard error, multiple correlation coefficient  $r$  and number of data points used in the calculation

	$\nu_0$	$s$	$a$	$b$	se	$r$	Data points
NBD-NHMe (1) <sup>a</sup>	20.06	-0.96	-0.27	-0.35	0.12	0.961	20
NBD-NHPh (2) <sup>a</sup>	19.47	-1.59	-0.19	-0.45	0.18	0.961	20
ABD-OMe (3) <sup>a</sup>	23.21	-1.47	-0.61	-0.57	0.23	0.950	20
DBD-OMe (4) <sup>b</sup>	22.84	-1.28	-0.38	—	0.36	0.795	20
ABD-SMe (5) <sup>a</sup>	21.21	-1.57	-0.44	-0.43	0.21	0.952	20
DBD-SMe (6) <sup>b</sup>	21.59	-2.00	-0.50	—	0.24	0.900	20

Calculations were performed using <sup>a</sup> eqn. (2) or <sup>b</sup> eqn. (3) to treat the whole set of data.

**Table 6** INDO/S results of the emission process for six benzofurazan compounds

	$\lambda_{em}/\text{nm}$	$f$	CI
NBD-NHMe (1)	541	0.286	HOMO→LUMO(94%)
NBD-NHPh (2)	556	0.327	HOMO→LUMO(94%)
ABD-OMe (3)	484	0.223	HOMO→LUMO(95%)
DBD-OMe (4)	484	0.226	HOMO→LUMO(95%)
ABD-SMe (5)	463	0.259	HOMO→LUMO(96%)
DBD-SMe (6)	446	0.279	HOMO→LUMO(95%)

$f$  = Oscillator strength.

**INDO/S calculation.** The electronic transition of the emission process from the lowest vibration  $S_1$  state to the ground state of the six 4,7-disubstituted benzofurazan compounds was studied by using INDO/S calculation and the results are summarized in Table 6. The INDO/S results of the energy gap between the HOMO and the LUMO (**1** 5.786 eV, **2** 5.697 eV, **3** 6.130 eV, **4** 6.120 eV, **5** 6.219 eV, **6** 6.209 eV) agreed with the fact that the emission wavelengths of NBD derivatives **1** and **2** were longer than ABD and DBD derivatives **3–6**. The agreement suggested that the maximum emission wavelengths of 4,7-disubstituted benzofurazan compounds are determined by the energy gap between the HOMO and LUMO energy at the optimized geometry of the lowest vibrational  $S_1$  state.

**PM3-CAS/CI calculation.** To elucidate the factor which determines the fluorescence quantum yield ( $\Phi$ ), the energy levels of the six 4,7-disubstituted benzofurazan compounds were studied using PM3-CAS/CI calculation. The fluorescence quantum yields ( $\Phi$ ) in cyclohexane, where there were little solvent effects, were used for discussion. The electronic distribu-

tions of the HOMO and LUMO obtained with PM3-CAS/CI were similar to those obtained with INDO/S and comparable to those obtained from the experimental data described above. Thus, PM3-CAS/CI also seems to be suitable for investigating the ground and excited states of the six 4,7-disubstituted benzofurazan compounds. The calculated energy levels of the six 4,7-disubstituted benzofurazan compounds are shown in Table 7. First, the probability of nonradiative transitions to the TICT state with twisting of the substituent group will be discussed since the transitions to the TICT state have been reported as the important nonradiative pathway even in non-polar solvents.<sup>5</sup> The influence of the twist of the NHMe, NHPh, OMe and SMe groups, which are planar to the benzofurazan skeleton at the optimized  $S_0$  geometry, on the  $S_1$  energy was studied for six 4,7-disubstituted benzofurazan compounds. The results calculated with PM3-CAS/CI were shown in Table 8. The twisting of the substituent group is not favorable for the six 4,7-disubstituted benzofurazan compounds, because the  $S_1$  energies of the twisted form are not smaller than those of the planar form. Next, the probability of another nonradiative transition will be discussed. The PM3-CAS/CI calculations showed that the  $S_1$  energy level of the six 4,7-disubstituted benzofurazan compounds are very close to the  $T_2$  (second excited triplet state) energy level (Fig. 3). Therefore we considered the energy gaps between the  $S_1$  and  $T_2$  states as the parameter to reflect the probability of  $S_1 \rightarrow T_2$  intersystem crossing and tried to relate the energy gaps between the  $S_1$  and  $T_2$  states with the fluorescence quantum yield ( $\Phi$ ) of six 4,7-disubstituted benzofurazan compounds in cyclohexane. The smaller energy gap of the optimized geometry of the lowest vibrational  $S_0$  and  $S_1$  states was selected for each compound in this study. The order of the energy gaps between the  $S_1$  state and the  $T_2$  state (**5** 0.462 eV > **6** 0.380 eV > **1** 0.230 eV > **4** 0.202 eV > **3** 0.137 eV) agreed

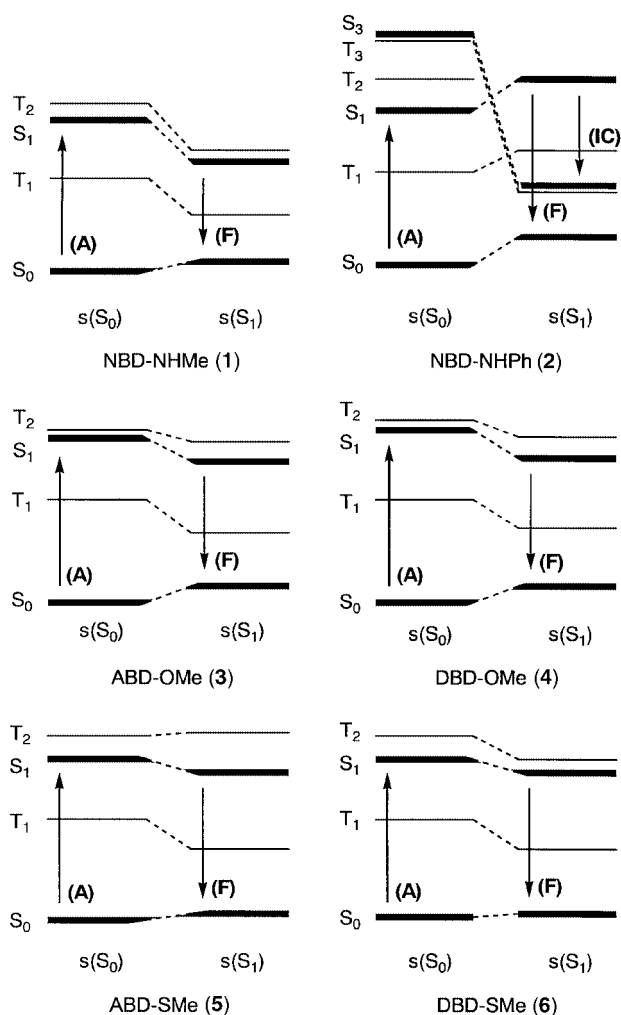
**Table 7** Results of PM3-CAS/CI calculation for six 4,7-disubstituted benzofurazan compounds

		CI Calculation for $s(S_0)^a$				CI Calculation for $s(S_1)^b$					
		Energy/eV	Multiplicity	Transition	State	$\Delta$ energy <sup>c</sup> /eV	Energy/eV	Multiplicity	Transition	State	$\Delta$ energy <sup>c</sup> /eV
NBD-NHMe (1)	1	-4.734	SINGLET	MO2→UMO1	S <sub>0</sub>		-4.619	SINGLET	MO2→UMO1	S <sub>0</sub>	
	2	-2.892	TRIPLET	MO2→UMO1	T <sub>1</sub>		-3.547	TRIPLET	MO2→UMO1	T <sub>1</sub>	
	3	-1.608	SINGLET	MO2→UMO2	S <sub>1</sub>	] $\Delta$ 0.322	-2.507	SINGLET	MO2→UMO2	S <sub>1</sub>	] $\Delta$ 0.230
	4	-1.286	TRIPLET	MO2→UMO2	T <sub>2</sub>		-2.277	TRIPLET	MO2→UMO2	T <sub>2</sub>	
NBD-NHPh (2)	1	-4.650	SINGLET	MO2→UMO1	S <sub>0</sub>		-4.087	SINGLET	MO1→UMO1	S <sub>0</sub>	
	2	-2.720	TRIPLET	MO2→UMO1	T <sub>1</sub>		-3.091	TRIPLET	MO1→UMO1	T <sub>3</sub>	
	3	-1.475	SINGLET	MO2→UMO1	S <sub>1</sub>	] $\Delta$ 0.753	-3.075	SINGLET	MO1→UMO1	S <sub>3</sub>	
	4	-0.722	SINGLET	MO2→UMO2	T <sub>2</sub>		-2.207	TRIPLET	MO2→UMO1	T <sub>1</sub>	
	5	-0.102	SINGLET	MO2→UMO2	S <sub>2</sub>		-1.428	TRIPLET	MO1→UMO2	T <sub>1</sub>	
	6	0.085	TRIPLET	MO1→UMO1	T <sub>3</sub>		-0.663	SINGLET	MO2→UMO1	S <sub>1</sub>	
	7	0.142	SINGLET	MO1→UMO1	S <sub>3</sub>						
ABD-OMe (3)	1	-5.109	SINGLET	MO2→UMO1	S <sub>0</sub>		-4.745	SINGLET	MO2→UMO1	S <sub>0</sub>	
	2	-2.911	TRIPLET	MO2→UMO1	T <sub>1</sub>		-3.532	TRIPLET	MO2→UMO1	T <sub>1</sub>	
	3	-1.551	SINGLET	MO2→UMO1	S <sub>1</sub>	] $\Delta$ 0.137	-2.117	SINGLET	MO2→UMO1	S <sub>1</sub>	] $\Delta$ 0.489
	4	-1.414	TRIPLET	MO1→UMO1	T <sub>2</sub>		-1.628	TRIPLET	MO1→UMO1	T <sub>2</sub>	
DBD-OMe (4)	1	-5.101	SINGLET	MO2→UMO1	S <sub>0</sub>		-4.712	SINGLET	MO2→UMO1	S <sub>0</sub>	
	2	-2.872	TRIPLET	MO2→UMO1	T <sub>1</sub>		-3.492	TRIPLET	MO2→UMO1	T <sub>1</sub>	
	3	-1.437	SINGLET	MO2→UMO1	S <sub>1</sub>	] $\Delta$ 0.202	-2.057	SINGLET	MO2→UMO1	S <sub>1</sub>	] $\Delta$ 0.548
	4	-1.235	TRIPLET	MO1→UMO1	T <sub>2</sub>		-1.509	TRIPLET	MO1→UMO1	T <sub>2</sub>	
ABD-SMe (5)	1	-4.726	SINGLET	MO2→UMO1	S <sub>0</sub>		-4.605	SINGLET	MO2→UMO1	S <sub>0</sub>	
	2	-2.593	TRIPLET	( $\pi$ → $\pi^*$ )	T <sub>1</sub>		-3.269	TRIPLET	( $\pi$ → $\pi^*$ )	T <sub>1</sub>	
	3	-2.433	TRIPLET	( $\pi$ → $\pi^*$ )	S <sub>1</sub>		-2.236	TRIPLET	( $\pi$ → $\pi^*$ )	S <sub>1</sub>	
	4	-1.564	SINGLET	( $\pi$ → $\pi^*$ )	T <sub>2</sub>	] $\Delta$ 0.462	-1.699	SINGLET	( $\pi$ → $\pi^*$ )	T <sub>2</sub>	] $\Delta$ 0.812
	5	-1.413	SINGLET	MO2→UMO1	S <sub>1</sub>		-1.695	SINGLET	MO2→UMO1	S <sub>1</sub>	
	6	-0.951	TRIPLET	MO1→UMO1	T <sub>2</sub>		-0.883	TRIPLET	MO1→UMO1	T <sub>2</sub>	
DBD-SMe (6)	1	-4.726	SINGLET	MO2→UMO1	S <sub>0</sub>		-4.606	SINGLET	MO2→UMO1	S <sub>0</sub>	
	2	-2.588	TRIPLET	( $\pi$ → $\pi^*$ )	T <sub>1</sub>		-3.264	TRIPLET	( $\pi$ → $\pi^*$ )	T <sub>1</sub>	
	3	-2.368	TRIPLET	( $\pi$ → $\pi^*$ )	S <sub>1</sub>	] $\Delta$ 0.462	-2.243	TRIPLET	( $\pi$ → $\pi^*$ )	S <sub>1</sub>	] $\Delta$ 0.380
	4	-1.512	SINGLET	( $\pi$ → $\pi^*$ )	T <sub>2</sub>		-1.698	SINGLET	( $\pi$ → $\pi^*$ )	T <sub>2</sub>	
	5	-1.402	SINGLET	MO2→UMO1	S <sub>1</sub>		-1.686	SINGLET	MO2→UMO1	S <sub>1</sub>	
	6	-0.940	TRIPLET	MO1→UMO1	T <sub>2</sub>		-1.306	TRIPLET	MO1→UMO1	T <sub>2</sub>	

<sup>a</sup>  $s(S_0)$  = the optimized geometry of the ground state. <sup>b</sup>  $s(S_1)$  = the optimized geometry of the excited state. <sup>c</sup>  $\Delta$  energy = the energy gap between the  $S_1$  and  $T_2$  states.

**Table 8** Effect of the twist of the substituent group on the  $S_1$  energy

Compound	Twisting group	$\Delta S_1/\text{eV}^a$
NBD-NHMe (1)	NHMe	0.539
NBD-NHPh (2)	NHPh	0.695
ABD-OMe (3)	OMe	0.248
DBD-OMe (4)	OMe	0.196
ABD-SMe (5)	SMe	0.676
ABD-SMe (6)	SMe	0.661

<sup>a</sup>  $S_1$  energy (twisted form) –  $S_1$  energy (planar form).**Fig. 3** Energy level diagrams for 4,7-disubstituted benzofurazan compounds obtained with PM3-CAS/CI calculation. (A) Absorption, (F) fluorescence, (IC) internal conversion.

approximately with the order of the fluorescence quantum yield ( $\Phi$ ) in cyclohexane ( $5 > 1 > 6 > 3 > 4$ ). This agreement indicated that the energy gap between the  $S_1$  and  $T_2$  states obtained with the PM3-CAS/CI calculations reflected the probability of the  $S_1 \rightarrow T_2$  intersystem crossing. The reasons why we considered that  $S_1 \rightarrow T_2$  intersystem crossing occurs under the condition that the  $T_2$  energy is higher than the  $S_1$  energy, are as follows. The energies of some of the excited molecules would be larger than not only  $S_1$  energies but also  $T_2$  energies at the optimized  $S_0$  geometry since the molecules are excited with vibrational energy to the higher  $S_1$  state. The ranges of absorption spectra of six 4,7-disubstituted benzofurazan compounds in cyclohexane proved that the molecules were excited to the  $S_1$  state higher than the  $S_1$  state at the  $S_0$  geometry. The ranges of absorption spectra (**1** 342–500 nm, **2** 342–521 nm, **3** 298–395 nm, **4** 299–400 nm, **5** 326–433 nm and **6** 319–430 nm, respectively) indicated that absorption energies are **1** 2.48–3.63

eV, **2** 2.38–3.63 eV, **3** 3.14–4.16 eV, **4** 3.10–4.15 eV, **5** 2.86–3.80 eV and **6** 2.88–3.89 eV respectively. Even if all the molecules are excited from the lowest vibrational  $S_0$  state, some of the molecules are excited to the  $S_1$  state higher than the  $T_2$  state (because the calculated  $S_0-T_2$  energy gaps at the  $S_0$  geometry are **1** 3.13 eV, **2** 3.18 eV, **3** 3.56 eV, **4** 3.66 eV, **5** 3.31 eV and **6** 3.32 eV respectively). Furthermore, the molecules may be excited to the  $S_1$  states higher than those estimated from the absorption energy since the molecules vibrate at the  $S_0$  state. In summary, the excited molecules have a larger  $S_1$  energy than the  $S_1$  energy at the  $S_0$  geometry because of the vibration. If the excited molecules with vibrational energy have a larger  $S_1$  energy than the  $T_2$  energy, intersystem crossing from the  $S_1$  state to  $T_2$  state would occur. On the other hand, if excited molecules have a smaller  $S_1$  energy than  $T_2$  energy, the  $S_1 \rightarrow T_2$  intersystem crossing would be precluded. Thus, the  $S_1-T_2$  energy gaps obtained with the PM3-CAS/CI calculations correlated well with the fluorescence quantum yields ( $\Phi$ ) of six 4,7-disubstituted benzofurazan compounds. These results are similar to the previous reports on monosubstituted anthracene compounds.<sup>27,28</sup> Exceptionally, the energy level of the  $S_1$  state and third excited singlet ( $S_3$ ) state of NBD-NHPh (**2**) at the optimized geometry of the lowest vibrational  $S_0$  state was reversed at the optimized geometry of the lowest vibrational  $S_1$  state, in which the benzene ring is approximately perpendicular to the benzofurazan ring like dinaphthylamine.<sup>29,30</sup> Therefore, the low fluorescence quantum yield ( $\Phi$ ) of NBD-NHPh (**2**) is presumed to derive from the internal conversion in addition to intersystem crossing.

## Conclusion

In this paper, we have tried to elucidate the factors which determine the fluorescence characteristics of six 4,7-disubstituted benzofurazan compounds and to clarify that the energy gap between the HOMO and LUMO at the geometry of the ground and excited states determine the maximum excitation/absorption wavelength and maximum emission wavelength, respectively. The fluorescence quantum yield ( $\Phi$ ) was also influenced by the frequency of occurrence of the intersystem crossing ( $S_1 \rightarrow T_2$ ) and internal conversion. Thus, this study showed for the first time that the semi-empirical molecular orbital calculation enables us to predict the fluorescence characteristics of 4,7-disubstituted benzofurazan compounds. In the future, the fluorescence characteristics of various solvents may be predicted by the energy gaps of HOMO–LUMO and  $S_1-T_2$  using the semi-empirical COSMO method. A similar approach using molecular orbital methods calculating the energy levels exactly might be applicable for studying the excitation and emission (relaxation) processes and make clear the factors which determine the fluorescence characteristics of a wider range of compounds.

## Experimental

### Materials

NBD-NHMe (**1**), NBD-NHPh (**2**), ABD-OMe (**3**), DBD-OMe (**4**), ABD-SMe (**5**) and DBD-SMe (**6**) were obtained according to the published procedures.<sup>18</sup> Propan-2-ol was obtained from Tokyo Kasei (Tokyo, Japan). Acetone, acetonitrile, *tert*-butyl alcohol, benzene, carbon tetrachloride, cyclohexane, dichloromethane, diethyl ether, dimethyl sulfoxide, 1,4-dioxane, ethanol, hexane, methanol, tetrahydrofuran and toluene were purchased from Kanto Chemicals (Tokyo, Japan). Chloroform, *N,N*-dimethylformamide and ethyl acetate were obtained from Wako Pure Chemicals (Osaka, Japan). Water was purified using a Milli-Q reagent system (Millipore, Bedford, MA, USA). All chemicals were of HPLC or guaranteed reagent grade and were used without further purification.

## Spectroscopic measurement

UV-VIS absorption spectra were measured on a JASCO (Japan Spectroscopic Co., Ltd.) Ubest-50 spectrometer (Tokyo, Japan) in various solvents (30  $\mu\text{M}$ ) at room temperature. Fluorescence spectra were measured on a Hitachi F-4010 fluorescence spectrometer (Tokyo, Japan) in various solvents (NBD-NHMe (1), 100 nM; NBD-NHPh (2), 30  $\mu\text{M}$ ; ABD-OMe (3), 1  $\mu\text{M}$ ; DBD-OMe (4), 30  $\mu\text{M}$ ; ABD-SMe (5), 1  $\mu\text{M}$ ; DBD-SMe (6), 2.5  $\mu\text{M}$ ) at room temperature. The emission spectra were obtained by exciting at the maximum absorption wavelengths. The fluorescence quantum yields ( $\Phi$ ) were determined using quinine sulfate in 0.1 M  $\text{H}_2\text{SO}_4$  ( $\Phi = 0.55$ , excitation wavelength: 355 nm, room temperature) as a standard.<sup>31</sup>

## Taft and Kamlet treatments<sup>32-34</sup>

The obtained maximum absorption wavelengths and maximum emission wavelengths in various solvents were analyzed with the Taft and Kamlet treatment. This treatment enables the solvatochromic shift attributable to hydrogen bonding to be disentangled from that attributable to non-specific solvent effects.

In the general expression (1),  $\nu_0$  is the vapor phase wave-

$$\nu = \nu_0 + s(\pi^* + d\delta) + aa + b\beta \quad (1)$$

number and the empirical parameters  $\pi^*$ ,  $a$  and  $\beta$  are a measure of the polarity/polarizability character of the solvent and of its hydrogen-bond donor and hydrogen-bond acceptor capacities, respectively. The coefficients  $s$ ,  $a$  and  $b$  indicate the susceptibility of  $\nu$  to a change in the corresponding parameter. The  $\delta$  parameter is a 'polarizability correction term', whose coefficient  $d$  is zero for all electronic spectra that are shifted bathochromically with increasing solvent dipolarity, as is the case for the 4,7-disubstituted benzofurazan compounds investigated here. Therefore we used eqn. (2) for the analysis of the

$$\nu = \nu_0 + s\pi^* + aa + b\beta \quad (2)$$

absorption and fluorescence of NBD-NHMe (1), NBD-NHPh (2), ABD-OMe (3) and ABD-SMe (5).

For compounds which are not hydrogen-bond donors, DBD-OMe (4) and DBD-SMe (6), using the  $\beta$ -scale was irrelevant, so the determination of  $\nu_0$ ,  $s$  and  $a$  was carried out using eqn. (3). The values of  $\pi^*$ ,  $a$  and  $\beta$ , cited from previous papers<sup>33,34</sup>

$$\nu = \nu_0 + s\pi^* + aa \quad (3)$$

are summarized in Table 9. All least-squares analyses were carried out with Microsoft EXCEL 97.

## Computational methods

Because of the large size of the six 4,7-disubstituted benzofurazan compounds, it was necessary to use semi-empirical methods in this study. All calculations were performed by means of PC-9821 Ls13. The semi-empirical calculation was carried out by the WinMOPAC ver. 2.0 package (Fujitsu, Chiba, Japan). Geometry calculations in the ground and excited states were carried out using the PM3 method.<sup>35,36</sup> Several starting geometries were used for the geometry optimization to ensure that the optimized structure corresponds to a global minimum. All geometries were completely optimized (keyword PRECISE, equivalent to GNORM =0.01 and SCFCRT =1.D-8) by the eigenvector following routine (keyword EF). Geometry in the excited states with a one-electron excitation from the HOMO to the LUMO was optimized with above keywords and keyword EXCITED.

Experimental absorption and emission spectra of the six 4,7-disubstituted benzofurazan compounds were studied with the semi-empirical method INDO/S (intermediate neglect of differential overlap/spectroscopic).<sup>37,38</sup> The parameter of sulfur atom

**Table 9**  $\pi^*$  Scale of solvent polarity,  $a$  scale of solvent hydrogen-bond donor acidities,  $\beta$  scale of solvent hydrogen-bond acceptor basicities and polarizability correction term  $\delta$

Solvent	$\pi^*$	$a$	$\beta$	$\delta$
<i>n</i> -Hexane	-0.11	0.00	0.00	0.00
Cyclohexane	0.00	0.00	0.00	0.00
Carbon tetrachloride	0.21	0.00	0.00	0.50
Diethyl ether	0.24	0.00	0.47	0.00
Toluene	0.49	0.00	0.11	1.00
Benzene	0.55	0.00	0.10	1.00
1,4-Dioxane	0.49	0.00	0.37	0.00
Chloroform	0.69	0.44	0.00	0.50
Dichloromethane	0.73	0.30	0.00	0.50
Ethyl acetate	0.45	0.00	0.45	0.00
Tetrahydrofuran	0.55	0.00	0.55	0.00
Acetone	0.62	0.08	0.48	0.00
Acetonitrile	0.66	0.19	0.31	0.00
<i>tert</i> -Butyl alcohol	0.41	0.68	1.01	0.00
Propan-2-ol	0.48	0.76	0.95	0.00
Ethanol	0.54	0.83	0.77	0.00
Methanol	0.60	0.93	0.62	0.00
<i>N,N</i> -Dimethylformamide	0.88	0.00	0.69	0.00
Dimethyl sulfoxide	1.00	0.00	0.76	0.00
Water	1.09	1.17	0.18	0.00

( $E_s = 21.02$   $E_p = 10.97$   $B_{sp} = 13.5$   $G = 10.01$ )<sup>39,40</sup> was added for the calculation of compounds 3-6. All INDO/S calculations were performed using single excitation full SCF/CI (self-consistent field/configuration interaction), which includes the configurations with one electron excited from any occupied orbital to any unoccupied orbital. All orbitals were used for CI calculations (keyword CI=all).

The energy levels of six benzofurazan compounds were calculated with the PM3-CAS (complete active space)/CI method. Four molecular orbitals were used for the PM3-CAS/CI calculation for NBD-derivatives 1 and 2 (keyword CI=4) and five molecular orbitals were used for ABD and DBD-derivatives 3-6 (keyword CI=5). Keyword "SINGLET ROOT=1" was also used for the calculation of the energy level at the structure of the lowest vibrational  $S_0$  state of the six 4,7-disubstituted benzofurazan compounds. The calculated energy levels of the singlet state resulting from the  $\pi \rightarrow \pi^*$  transition were assigned to  $S_0$ ,  $S_1$ ,  $S_2$ ,  $S_3$  in ascending order. Similarly, the calculated energy levels of the triplet state resulting from the  $\pi \rightarrow \pi^*$  transition were assigned to  $T_1$ ,  $T_2$ ,  $T_3$  in ascending order. The energy of each singlet and/or triplet state was corrected with the energy of the lowest vibrational  $S_0$  state calculated with keywords "EXCITED SINGLET ROOT=1" For the calculation of the energy level at the optimized geometry of the lowest vibrational  $S_1$  state of compounds 1-4, keyword "EXCITED SINGLET ROOT=2" were used. For the calculation of the energy level at the optimized geometry of the lowest vibrational  $S_1$  state of compounds 5 and 6, keyword "EXCITED SINGLET ROOT=3" were used, because "ROOT=2" corresponded to  $\pi \rightarrow \pi^*$  transition. The energy levels calculated at the optimized geometry of the excited state ( $S_1$ ) were assigned to the corresponding energy levels at the optimized geometry of the ground state ( $S_0$ ) with the agreement of the electron distribution before and after the transition.

## Acknowledgements

The authors thank Dr Chang-Kee Lim, MRC Toxicology Unit University of Leicester for his valuable suggestion and discussion.

## References

- 1 T. Foster, *Naturwissenschaften*, 1946, **33**, 220.
- 2 F. W. D. Rost, *Fluorescence Microscopy*, vol. 1, Cambridge University Press, Cambridge, 1992, p. 28.

- 3 E. L. Wehry and L. B. Rogers, *Fluorescence and Phosphorescence Analysis*, Wiley, New York, London and Sydney, 1966, p. 89.
- 4 D. S. McClure, *J. Chem. Phys.*, 1949, **17**, 905.
- 5 W. Rettig and A. Klock, *Can. J. Chem.*, 1985, **63**, 1649.
- 6 A. Takadate, T. Masuda, C. Murata, A. Isobe, T. Shinihara, M. Irikura and S. Goya, *Anal. Sci.*, 1997, **13**, 753.
- 7 H. Matsunaga, T. Santa, T. Iida, T. Fukushima, H. Homma and K. Imai, *Analyst*, 1997, **122**, 931.
- 8 G. Jones II, W. R. Jackson and A. M. Halpern, *Chem. Phys. Lett.*, 1980, **72**, 391.
- 9 E. M. Kosower, *Acc. Chem. Res.*, 1982, **15**, 259.
- 10 R. Saito, T. Hirano, H. Niwa and M. Ohashi, *J. Chem. Soc., Perkin Trans. 2*, 1997, 1711.
- 11 S. Otsuki and T. Taguchi, *J. Photochem. Photobiol. A: Chem.*, 1997, **104**, 108.
- 12 K. Imai and Y. Watanabe, *Anal. Chim. Acta*, 1994, **290**, 3.
- 13 T. Toyo'oka, T. Suzuki, Y. Saito, S. Uzu and K. Imai, *Analyst*, 1989, **114**, 413.
- 14 T. Toyo'oka and K. Imai, *Anal. Chem.*, 1984, **56**, 2431.
- 15 K. Imai, T. Toyo'oka and Y. Watanabe, *Anal. Biochem.*, 1983, **128**, 471.
- 16 T. Santa, K. Kimoto, T. Fukushima, H. Homma and K. Imai, *Biomed. Chromatogr.*, 1996, **10**, 183.
- 17 T. Santa, A. Takeda, S. Uchiyama, T. Fukushima, H. Homma, S. Suzuki, H. Yokosu, C. K. Lim and K. Imai, *J. Pharm. Biomed. Anal.*, 1998, **17**, 1065.
- 18 S. Uchiyama, T. Santa, T. Fukushima, H. Homma and K. Imai, *J. Chem. Soc., Perkin Trans. 2*, 1998, 2165.
- 19 S. Uchiyama, T. Santa and K. Imai, *J. Chem. Soc., Perkin Trans. 2*, 1999, 569.
- 20 H. Heberer and H. Matschiner, *J. Prakt. Chem.*, 1986, **328**, 261.
- 21 S. Lin and W. S. Struve, *Photochem. Photobiol.*, 1991, **54**, 361.
- 22 S. F. Forgues, J. P. Fayet and A. Lopez, *J. Photochem. Photobiol. A: Chem.*, 1993, **70**, 229.
- 23 G. Jones II, W. R. Jackson, C. Choi and R. Bergmark, *J. Phys. Chem.*, 1985, **89**, 294.
- 24 S. F. Forgues, C. Vidal and D. Lavabre, *J. Chem. Soc., Perkin Trans. 2*, 1996, 73.
- 25 W. Rettig, *Angew. Chem., Int. Ed. Engl.*, 1986, **25**, 971.
- 26 J. A. V. Gompel and G. B. Schuster, *J. Phys. Chem.*, 1989, **93**, 1292.
- 27 R. E. Kellog, *J. Chem. Phys.*, 1966, **44**, 411.
- 28 R. G. Bennett and P. J. McCartin, *J. Chem. Phys.*, 1966, **44**, 1969.
- 29 J. Dresner, S. H. Modiano and E. C. Lim, *J. Phys. Chem.*, 1992, **96**, 4310.
- 30 D. Chen, R. Sadygov and E. C. Lim, *J. Phys. Chem.*, 1994, **98**, 2018.
- 31 A. N. Fletcher, *Photochem. Photobiol.*, 1969, **9**, 439.
- 32 M. J. Kamlet, J. L. M. Abboud, M. H. Abraham and R. W. Taft, *J. Org. Chem.*, 1983, **48**, 2877.
- 33 C. Laurence, P. Nicolet, M. T. Dalati, J. L. M. Abboud and R. Notario, *J. Phys. Chem.*, 1994, **98**, 5807.
- 34 Y. Marcus, *J. Soln. Chem.*, 1991, **20**, 929.
- 35 J. J. P. Stewart, *J. Comput. Chem.*, 1989, **10**, 209.
- 36 J. J. P. Stewart, *J. Comput. Chem.*, 1989, **10**, 221.
- 37 J. Ridley and M. Zerner, *Theor. Chim. Acta*, 1973, **32**, 111.
- 38 J. Ridley and M. Zerner, *Theor. Chim. Acta*, 1976, **42**, 223.
- 39 D. J. Sandman, G. P. Ceasar, A. P. Fisher III, E. Schramm, D. D. Titus and A. D. Baker, *Chem. Mater.*, 1989, **1**, 421.
- 40 H. Baumann, CNDUV99, *Quantum Chemistry Program Exchange*, #333.

Paper 9/04989D